Characteristics of Prototype Silicon Sensors for Run2b (II)

N. Bacchetta[1], G. Bolla[4], D. Bortoletto[4], A. Canepa[4], B. Flaugher[1], I. Gorelov[3], K. Hara[5],
M. Hoeferkamp[3], D. Pellett[2], S. Seidel[3], Y. Takei[5], P. Watje[3]

[1]Fermilab, Batavia, Illinois, USA
[2]University of California, Davis, California, USA
[3]University of New Mexico, Albuquerque, New Mexico, USA
[4]Purdue University, West Lafayette, Indiana, USA
[5]University of Tsukuba, Tsukuba, Ibaraki, Japan

Abstract

Five prototype silicon sensors were irradiated with neutrons up to 1.4×10^{14} n/cm^2, as a part of the sensor quality assurance program for Run2b silicon detector. This note describes the characteristics of irradiated sensors. We comment on charge-up susceptibility of the new sensors which employ wafers in <100> direction.

1. Introduction

The prototype sensors are AC coupled and single-sided, which are designed to have lifetime extending to the end of Run2b. Due to the intense radiation, the full depletion voltage will, after type inversion, increase up to about 200V (100V) at 15 fb^{-1} and to 380V (200V) at 30 fb^{-1} for the L0 (L1) sensors located 2 cm (3 cm) from the collision point. These estimates include a safety margin of 1.5 in the radiation fluence. The corresponding 1 MeV equivalent neutron fluence at L0 is 1.4×10^{14} n/cm^2 after 30 fb^{-1}. This note describes the electrical performance of five sensors irradiated with neutrons. The evaluations were performed at three universities, Tsukuba, Purdue and New Mexico. Characteristics of non-irradiated sensors are reported in CDF note 6286.

Long-term stability tests have been initiated to test the leakage current stability and durability of the coupling capacitors. The status results are presented.

In the early stage of testing, we experienced some charge up problem. The present sensors which employ <100> wafers seem to have more susceptibility than for <111> wafers. Some preliminary observations to understand this phenomenon are described.

2. Performance of Neutron-Irradiated Sensors

2.1 Neutron Irradiation

We have irradiated 5 prototype sensors with neutrons at MNRC Irradiation Facility at UC Davis on September 27, 2002. Three of the sensors (Sensor Number 060, 063, 069) received 1.4×10^{14} cm^{-2} 1-MeV neutron equivalent fluence and the other two (Sensor Number 001, 002)

0.7×10^{14} cm^{-2} 1-MeV equivalent. The irradiation time was 69 min in total. The actual doses[1] evaluated by sulfer activation are $(0.67 \pm 0.02) \times 10^{14}$ and $(1.40 \pm 0.02) \times 10^{14}$ n/cm^2.

The irradiated sensors were stored at a low temperature (-7°C). The sensor temperature was then increased for certain periods so that the sensors should almost complete the initial annealing and to have the full depletion voltage almost at the minimum. The three sensors irradiated to 1.4×10^{14} n/cm^2 were characterized at Purdue, and the two irradiated to 0.7×10^{14} n/cm^2 at UNM and Tsukuba.

Characterization of irradiated sensors is not straightforward due mainly to existence of large surface charges and total leakage current. One guideline is to cool down the sensors to be sensitive to the intrinsic properties which we want to evaluate. Tsukuba and Purdue Groups have used environment chambers for this purpose. Connections to only limited number of channels were provided by wire-bonding. Purdue Group has used in addition a cooled chuck so that probing is still possible. UNM Group has measured quickly at room temperature, and sent the samples to Tsukuba Group for further testing.

2.1 Total Leakage Current

Figure 1a shows I-V curves of three sensors irradiated to 1.4×10^{14} n/cm^2 measured at 13°C but the currents are renormalized at 20°C. The three sensors have been annealed at room temperature for 1700 min (060), 1200 min (063) and 2800 min (069). Sensor 069 has experienced additional annealing at higher temperature (4 min at T=80°C) to complete the initial annealing, which explains smaller leakage current than others. Figure 1b shows I-V curves of one of the sensors (002) irradiated to 0.7×10^{14} n/cm^2. The temperatures were in the range –30 to –10°C. This sensor was kept at room temperature so that the initial annealing should have completed. The two sensors 063 and 069 showed a gradual leakage current increase at 490 V and 180V, respectively,
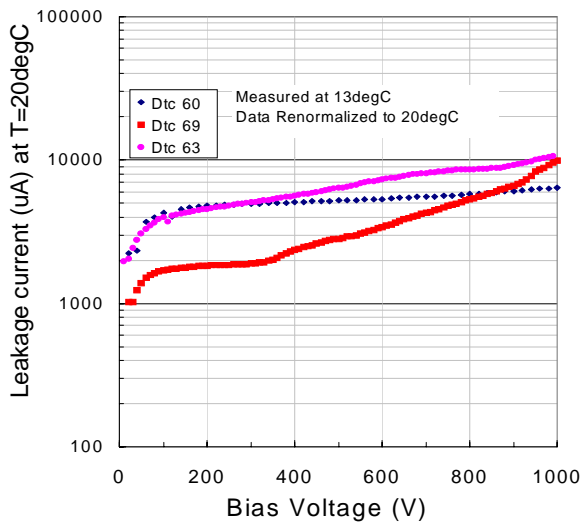

Fig. 1a I-V curves of three sensors irradiated to 1.4×10^{14} n/cm^2. The data are renormalized to T=20°C. Note different annealing time for 69 (see text).

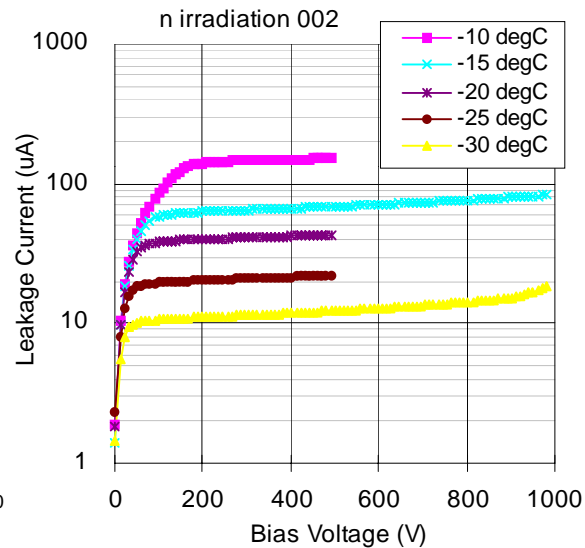Fig. 1b I-V curves of a sensor irradiated to 0.7×10^{14} n/cm^2. HV was raised to 1 kV only at –15 and –30°C.

---

[1] The error does not account for the error in sulfer activation cross section. Also, the uncertainty arising when translating the damage at different energies to that at 1 MeV is not added: The neutron energy spectrum has a peak at 1 MeV, ranging from 1 eV to 10 MeV.

before irradiation. As shown in Fig. 1a the onset voltage of Sensor 069 is shifted toward higher voltage 350V. It is not very distinct for 063 since the increase is moderate. We note that 060, 002 and 001 (not shown) have I-V curves extending to 1000V without any micro-discharge.

Previous studies have shown that the leakage current of irradiated sensors decreases (annealing) with time approaching to an asymptotic value. The damage constant α is expressed by $\alpha = \phi \cdot \Delta I / V$, where ϕ is the neutron fluence, ΔI is the increase in the total leakage current measured at full depletion voltage, and V is the volume of the sensor. Because of the features of annealing and temperature dependence of the leakage current, α is usually calculated after the annealing is almost completed and at 20°C.

Systematic study of the annealing phenomena is available such as from Rose Collaboration. At room temperatures, the current decreases substantially within a month, approaching to an asymptotic damage constant of 3×10^{-17} A/cm.

The present results are used to evaluate the neutron fluence. Using 069, which has been annealed extensively, the fluence is evaluated to 1.1×10^{14}/cm^2 for nominal of 1.4×10^{14}/cm^2. Similarly with use of 001 and 002, and other data measured at different annealing, the neutron fluence is evaluated to $(0.33-0.64) \times 10^{14}$/cm^2 for nominal of 0.7×10^{14}/cm^2. The present results prefer somewhat smaller neutron fluence but are in reasonable agreement.

2.2 Full Depletion Voltage

The measurement of full depletion voltage is strongly affected by high leakage current and therefore is performed in the environmental chamber at –25°C. For Sensor 060, the LCR is set to f=1kHz and V_{AC}=1V, and the full depletion voltage is calculated from the $1/C^2 - V_{bias}$ plot. The obtained value is then normalized to the nominal frequency and temperature f=10kHz and T=20 $^{\circ}$C (ROSE/TN/2000-10). The normalized full depletion voltage is 128 V. Sensor 063 showed similar value of 130 V.

The curves for 0.7×10^{14}/cm^2 sensors are taken with the LCR frequency of 100 Hz. Since the curves are quite dependent on the temperature and somewhat on the LCR frequency, we do not quote the full depletion voltage. The two sensors, though, show a full depletion consistent with around 50V.

Time evolution of the full depletion voltage is calculated using the parameters given by ROSE Collaboration. Appendix summarizes the equations and the parameters we used, where the plots are also given. In the present calculation, we assume that the initial full depletion voltage is 150 V and the sensors are irradiated to equivalent neutron fluence of 0.7×10^{14}/cm^2 or 1.4×10^{14}/cm^2. We expect that the full depletion voltage be around 40V and 120V, respectively.
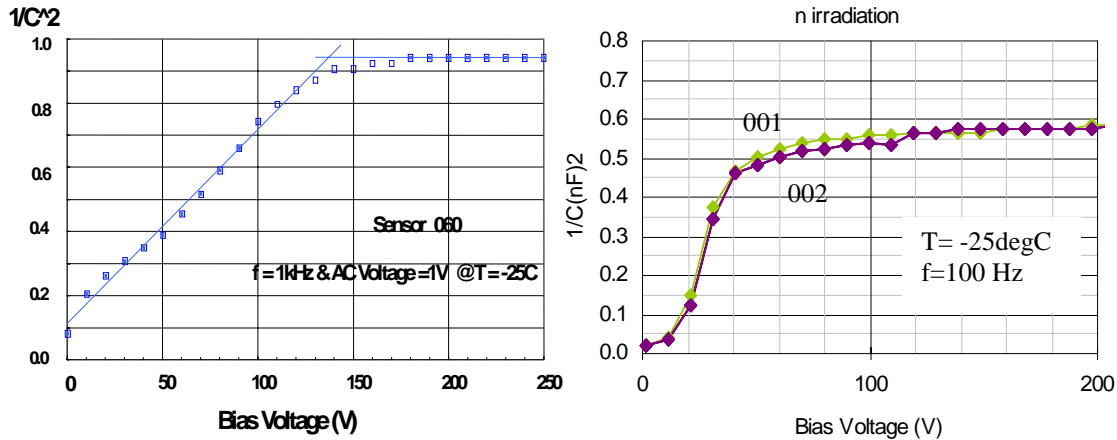

Fig. 2 $1/C^2$-V curves of n-irradiated sample. (Left) 060 Sensor and (Right) 001/002 Sensors. Note the difference of C at plateaux is due to the frequency settings.

2.3 Poly-silicon Resistance

The poly-silicon resistance is measured and compared before and after irradiation. Figure 3 shows the bias dependence measured for a particular strip. Although the resistance is set saturated at about 100V before irradiation, it requires much larger bias voltage, about 350V, to reach the saturated value. The intrinsic poly-silicon should not be degraded but the surface charge obviously degrades the isolation after irradiation. The measured poly-silicon resistance after irradiation seems slightly smaller. Again, we interpret this is due to that the surface isolation is degraded. In any case the changes are small and acceptable.
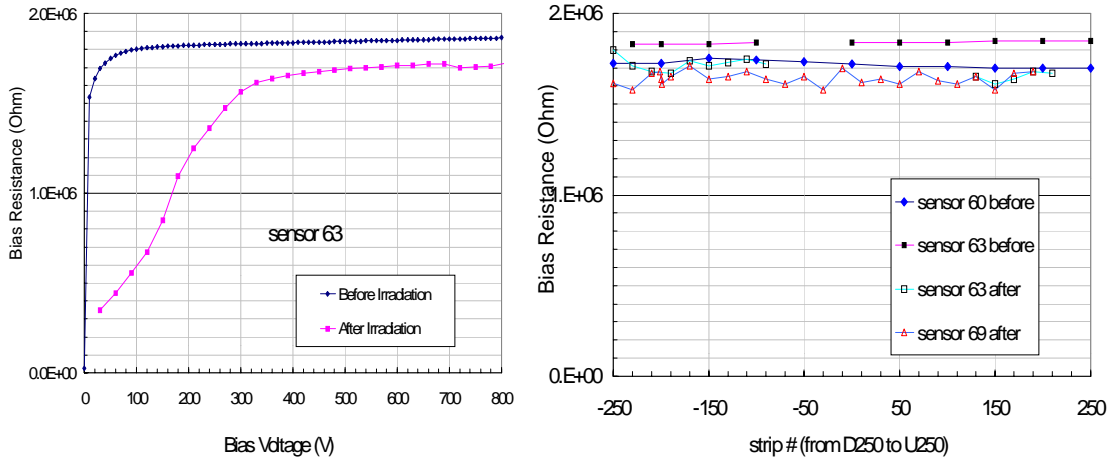
Fig. 3 (Left) Bias resistance measured as a function of bias.(Sensor 063) . (Right) Bias resistance versus strip number.

2.4 Interstrip Resistance

The interstrip resistance is one of the key parameters to evaluate the radiation effect on silicon detectors. The oxide layer between strips accumulates positive charges created due to radiation, which degrades the interstrip resistance.

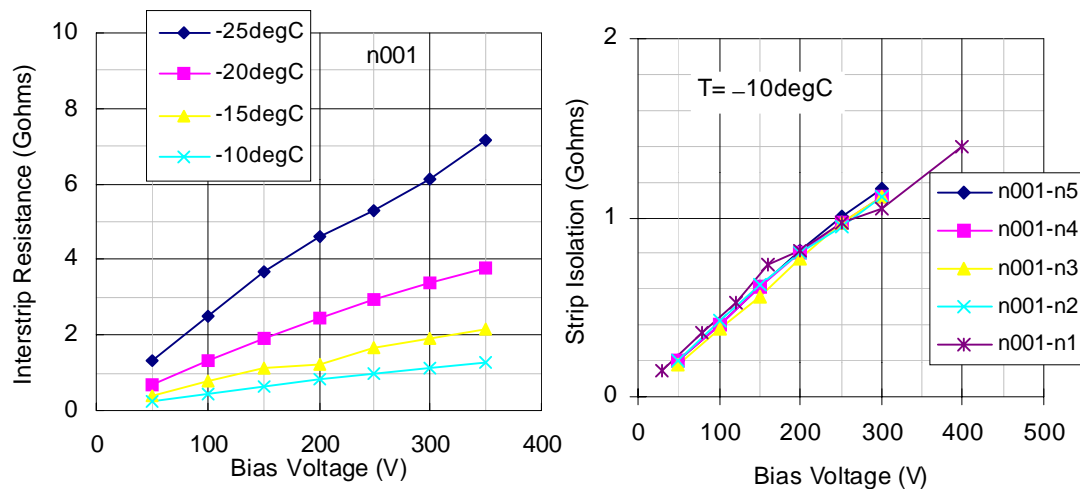Figure 4a shows bias dependence of the resistance. The plots show the temperature dependence

Fig. 4b Interstrip resistance as a function of bias voltage. (Left) Temperature dependence measured for 001 Sensor. (Right) channel dependence measured at -10°C.

(Sensor 001) and variations among strips (Sensor 001) measured at –10°C. The resistance is substantially degraded: it is greater than 40 GΩ before irradiation. In order to keep the resistance to be more than 1G Ω, bias of 250V (50V) is required at –10°C (–25°C). Since the oxide charge plays the essential role whose effects should be larger at higher temperatures, we have to respect the temperature where we evaluate the interstrip resistance. Although the bias voltage 250V is substantially larger than the full depletion voltage of 50V, where we naively expect that the strips are isolated, the required voltage is small enough and manageable.

2.5 Interstrip Capacitance

Figure 5a shows the bias dependence of the interstrip capacitance measured for particular sets of neighboring strips. The LCR frequency is 1 MHz. The shoulders around 130V are consistent with the full depletion voltage. The interstrip capacitance decreases gradually with bias voltage, approaching to asymptotic values consistent with those of non-irradiated sensors. The asymptotic value is 3.3 pF (3.17 pF) for Sensor 063 (Sensor 060), which is to be compared with 3.4 pF (3.46 pF) obtained before irradiation. We notice, though, that the bias should be substantially larger than the full depletion voltage to reach the asymptotic value.
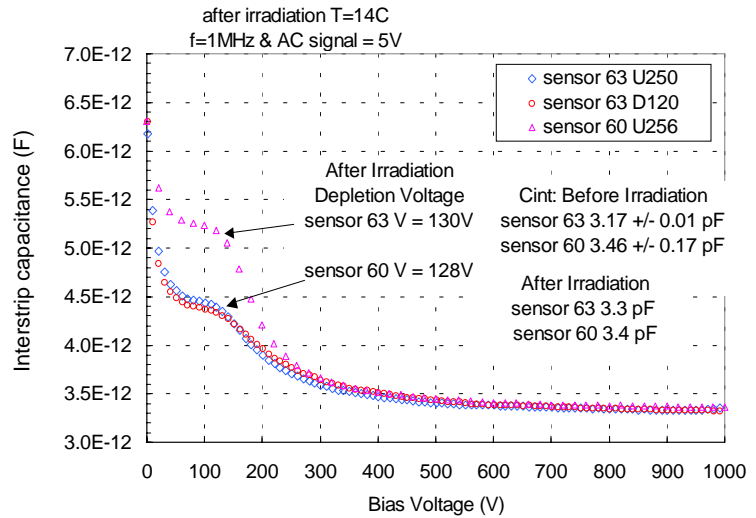

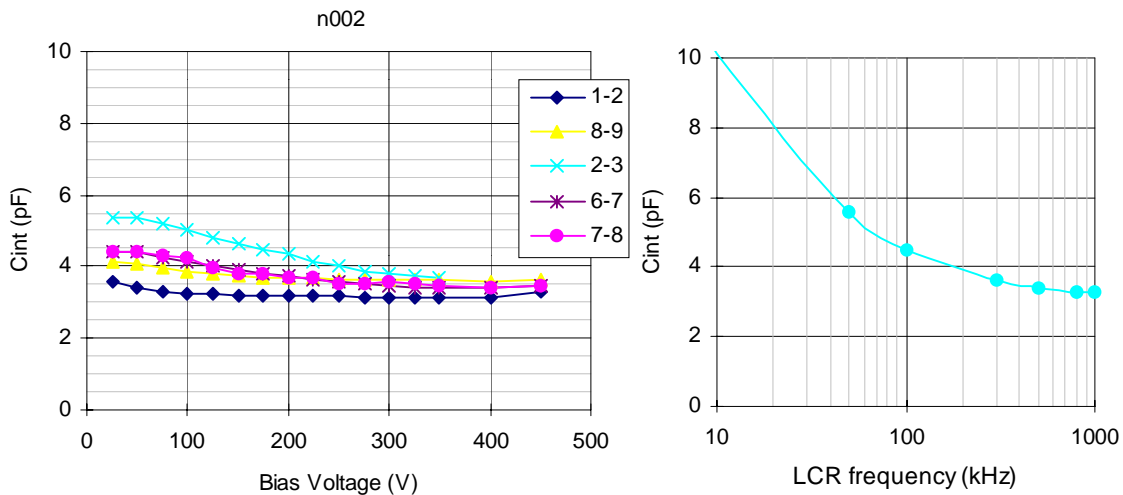Fig. 5a Interstrip capacitance of irradiated 063 and 060 sensors, measured as a function of bias voltage.

Fig. 5b (Left) Interstrip capacitance for sampled strips of Sensor 002. The LCR frequency is 1MHz. (Right) Frequency dependence of interstrip capacitance at bias of 300V. The temperature is –25°C.

Figure 5b shows the interstrip resistance of Sensor 002 measured as a function of bias with LCR frequency of 1 MHz. Again, a bias substantially larger than the full depletion voltage (about 50V) is required to reach the asymptotic value. From the frequency dependence, measured at bias voltage of 300V, it is still possible that the interstrip capacitance decreases further if the LCR frequency is raised.

2.6 Coupling Capacitance

Figure 6 shows the uniformity of the coupling capacitance measured after irradiation. The data are shown for two sensors. The average values measured on Sensor 060 and 069 are 136.3 ± 1.2 (134.4 ± 0.5) pF and 134.5 ± 5.3 (126.5 ± 1.0) pF after (before) irradiation. The data before and after are comparable for both sensors. Similarly, essentially no degradation is observed also for Sensor 001 and 002.
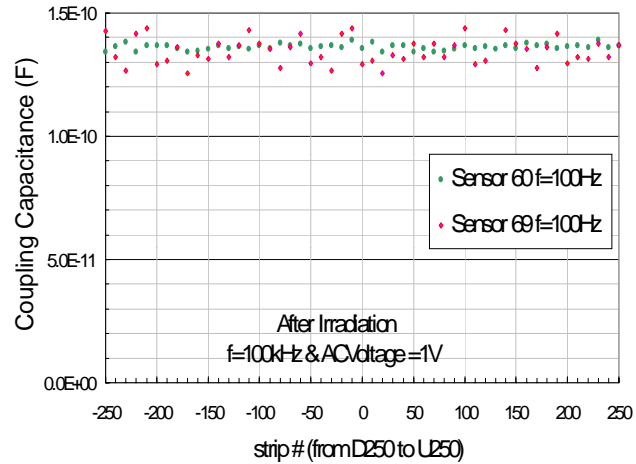

Fig. 6 Coupling capacitance versus strip number, measured for Sensor 060 and Sensor 069.

2.7 Summary of Irradiation Tests

We have characterized various electrical parameters of the sensors irradiated with neutrons up to $1.4 \times 10^{14} n/cm^2$. The full depletion voltages are uniform among the samples irradiated to the same dose, and are consistent with previously known values. Many parameters such as interstrip capacitance, interstrip resistance, and bias resistance are apparently degraded to some extent due to positive charges accumulated in oxide layer and type inversion.

The *p+* strips are in the ohmic contact side after the bulk is inverted to *p* type. The strips are not well isolated unless the bulk is fully depleted. However, we expect that the interstrip capacitance and other parameters should reach rapidly the asymptotic values if the bias exceeds the full depletion voltage. Our observation is that this transient is moderate and it requires additional voltage to reach the asymptotic value. Consequently, we need to set the bias at substantially larger than the full depletion voltage to obtain best detector performance. Typically a bias of 250-300V is required for the depletion voltage of around 130V.

Hamamatsu sensors, which show superior durability against high voltages, are best suited for our application, and fulfill the specifications required for Run2b Detector.

3. Long-term stability tests

The long-term stability tests have been initiated at Tsukuba and UNM. At Tsukuba, eight sensors (4 axial and 4 stereo sensors) are biased for nearly two months. The bias-ring and Nsub pad, a pad resistively coupled to the back-plane, are wire bonded to external traces to which +500V is applied with the bias-ring at ground. In addition, in order to test the oxide durability, 30 AC pads per sensor are wire-bonded to an external electrode to which +100V is applied. The setup is placed in an environment chamber at 20°C. At UNM, two axial sensors are biased. The stability test consists of two one-week long sets, one set for coupling capacitance durability where 120V was applied across the DC and AC pads of adjacent four strips, and another set for leakage current stability where 500V was applied between the back-plane and the bias-ring.

3.1 Leakage Current Stability

The leakage current stability data obtained by Tsukuba Group are shown in Fig. 5a. The data were taken typically once per day. When Vcp (=100V) is applied across the AC pad and the implant electrode, the total leakage current increases substantially, typically to 100 μA whereas the leakage current without Vcp is less than 1 μA. Actually this increase, evident for Vcp above 80V, is reproducible and uniform among the eight sensors. We employ extended Al electrode structure, which makes the electric field at this region strong and initiates micro-discharge. Therefore, we set Vcp to zero when we take the leakage current data. Since Dec 7, we decided to turn off Vcp for typically 1 hr prior to the leakage current measurement. After that the leakage current became fairly stable.

The stability data obtained by UNM Group are shown in Fig. 5b, where temperature data are plotted together. We observe that the leakage current of both sensors tracks very closely the variances in temperature, and that when the temperature is fairly stable so is the value of sensor leakage.

Comparing the two results, we notice that the Tsukuba sensors are less stable. Also some of sensors, e.g. S23 and A54, have a tendency to increase the leakage gradually. Such a variation could be explained by fluctuation of micro-discharge onset voltage. However, we measured I-V curves and observed that no sensors show micro-discharge up to 1000V. We suspect that edge current may be continuously high as Nsub pad is used for biasing.
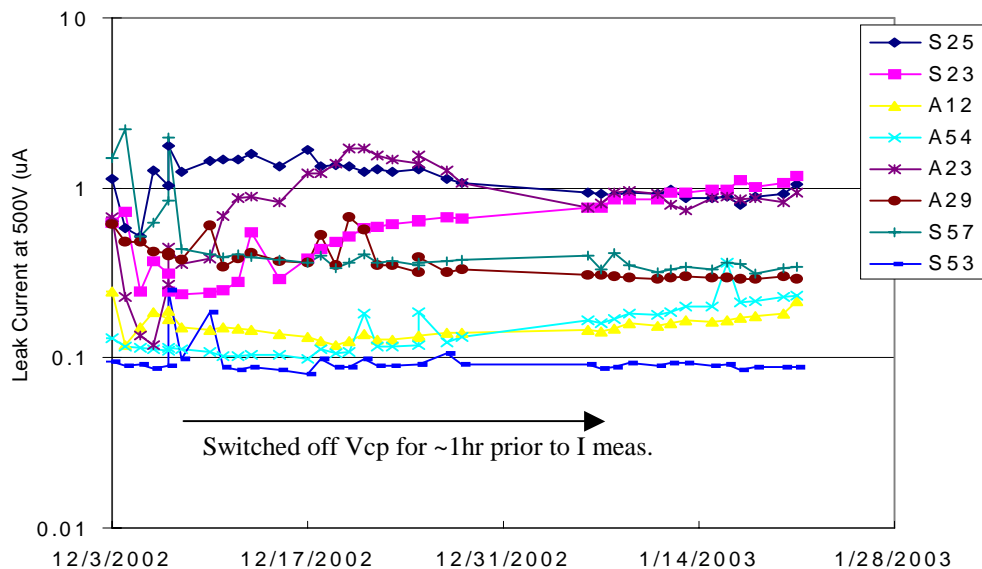

Fig. 5a Leakage current stability for eight sensors biased at 500V. Note the change in the measurement procedure (see text) after 2002/12/07.
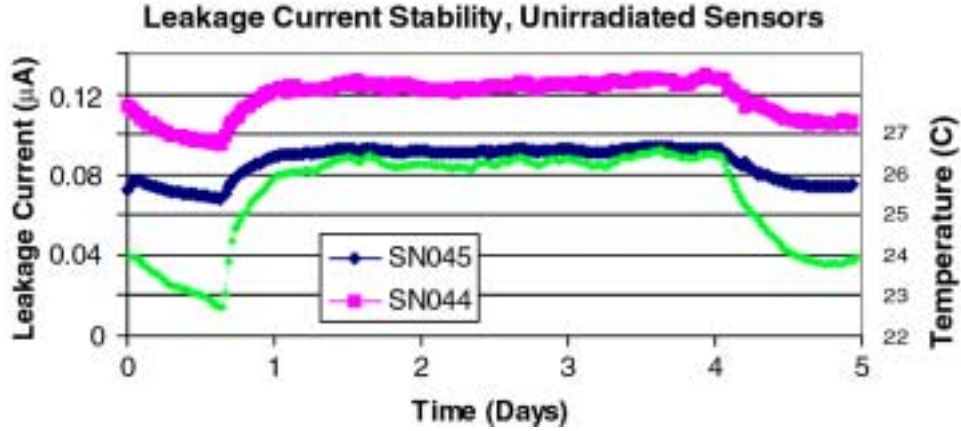
Leakage Current Stability, Unirradiated Sensors

Fig. 5b Leakage current stability for two sensors. The temperature (RHS) is shown in green.

3.2 Coupling Capacitor Stability

The coupling oxide punch-through is specified not to occur below 100V. Although, in our application, no voltage is applied to the oxide, this requirement is retained in engineering point of view to ensure that the process is properly completed: HPK oxide layers should stand up to 100V. HPK applies 120V across the oxide for 1/6 sec (actually they do twice, so in total 1/3 sec) in order to ensure the durability at 100V for years.

The coupling capacitor stability is measured to find out how robust the coupling capacitors are when subjected to worst case conditions, applying 120V between the AC and DC pads. Four adjacent strips are ganged together. The results are shown in Fig. 6c, where the leakage current with the applied voltage is seen to be much less than the 1 nA level. Figure 6d plots the values of the four coupling capacitors which had the 120V potential applied, along with their neighbors. A decrease of approximately 1.5% is seen. It is possible that our measurement, made 0.5 h after switching off the 120V, have recorded transient values before the oxide condition is stabilized.

Among the eight sensors with 100V applied for nearly two months, one axial sensor A23 failed after one day due to punch-through. This is unfortunate but HPK testing of axial sensors was incomplete (See CDF 6286) to ensure 100V durability. Since then, no other sensor showed creation of punch-through.
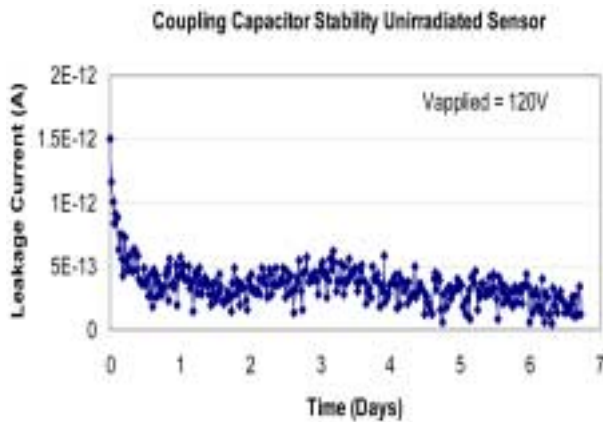

Fig. 6c Leakage current through four coupling capacitors at neighbor. 120V is applied across the coupling capacitors. The temperature was stable within 2°C during this test.
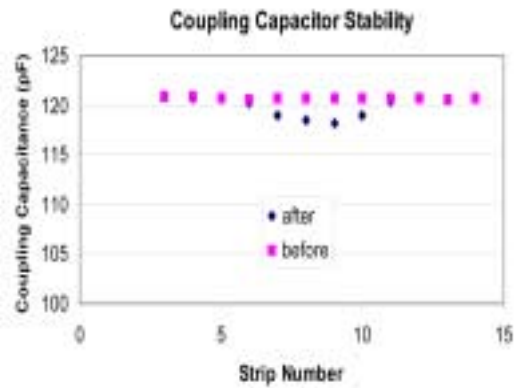
Fig. 6d Coupling capacitance values compared before and after the 7-day durability test. The central four strips had 120V on them.

4. Effects of Charge-up

In early stage of testing, we recognized that the sensors are easier to charge up compared to ISL/L00 sensors. This tendency was observed at Tsukuba and Purdue (UNM recorded some hint of the effect). Figure 10a is an example of such data obtained at Tsukuba. In this case, typically 30-40 central strips showed smaller resistances (R in the figure). Also some non-uniformity is seen for the coupling capacitors (Ccp) in the same region. From the location and spread, Tsukuba Group suspected that the vacuum tweezers used to pick up the sensor was causing the trouble. After eliminating use of tweezers, this effect turned to be hard to appear[2].
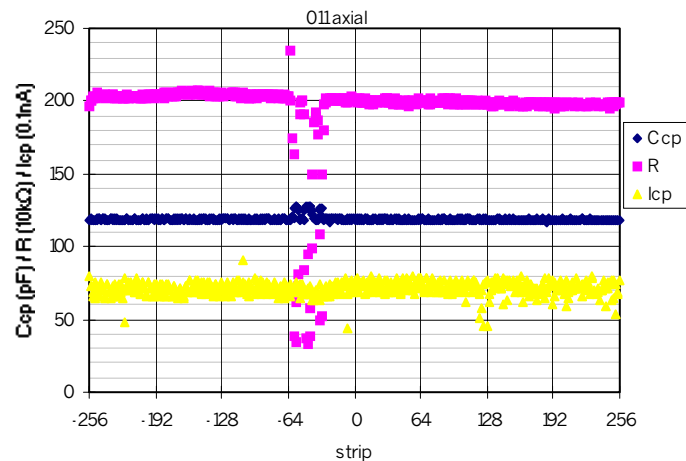

Fig.10a Example AC scan plot for a sensor with charge-up.

The charge-up mechanism can be explained that a thin p-type layer, an inversion layer, is created on the surface of n-type bulk by external static charges. This deteriorates the electrical isolation between strips, which was actually identified from strip isolation test as well. This type inversion is easier to occur for <100> than for <111> because the positive charge trapped at the Si-SiO_2 interface and fixed oxide charge in SiO_2 layer are about one order abundant for <111>[3]. This explains qualitatively why we did not see charge-up for ISL/L00 sensors, which employ <111> wafers. It is important to note that HPK is checking the isolation for every strip. This insures that the isolation degradation must have occurred during handling. Actually all the sensors have recovered from charge-up when they were placed back in the envelope which is used by HPK at sensor delivery. But it is also the observation that the charge-up can remain for long time if the sensor is just kept on the test stage.

The inversion layer could remain for a long time if there is no route for the charges to move. In our detector application, though, there are a couple of routes possible: (1) Al electrodes are connected to ASICs, (2) Signal currents are created by particles passing through, and (3) Positive ions are accumulated in oxide layer due to radiation. The positive ions (3) attract electrons at the oxide-silicon boundary, thus removing the inversion layer.

Purdue Group observed irregular resistance values for one sample. This sample was then irradiated with neutrons. As shown in Fig. 10b, a cluster of strips which initially showed small resistance have recovered to nominal resistance after irradiation. Although it is probable that charge up effect disappeared by other effects, an assumption is that positive charge trapped in the silicon dioxide helped to diminish the inversion layer ((3) described above).

We have made several tests such as to investigate time constants for the inversion layer to disappear. The tests included studying the effect of wire-bonding simulating the connection to ASICs, of epoxy applied on the surface for hybrid gluing, and of UV illumination. Preliminary observations we have are:

 (1) Inversion layers seem to diminish quickly if the sensors are wire-bonded.

---

[2] Four consecutive sensors showed similar effects before Tsukuba Group stopped using tweezers. Since then, we observed degraded isolation for a couple of strips but much less frequently. We suspect probe tips which were not properly discharged before use caused this. Recently, in order to carry out the study described here, we are back to use the same tweezers to intentionally reproduce charge-up sensor but failed.
[3] See, for example, S. M. Sze, "Semiconductor Devices": John Wiley & Sons 1985.

(2) If the sensors are not wire-bonded, the surface charge could remain at least for days.

(3) Removal of inversion layer is accelerated if the sensor is illuminated with UV.

(4) Epoxy on the surface helps to remove the charge, but too much epoxy degrades the surface isolation, which in turn makes the sensor easily affected by external conditions.

The above are preliminary since the study is not complete. We tried to carry out more systematic studies, but failed to do because we have not succeeded to reproduce charge-up sensors. Comparing the easiness of charge-up we encountered at earlier time, the sensors, three months after delivery, must have changed the susceptibility. One of such changes could be that oxide layer has accumulated positive charges enough to prevent the sensor from charge-up.

Fig.10a Poly-silicon resistance versus strip number. While some irregular values before irradiation (blue circles) indicate existence of charge up, the resistance is uniform after irradiation (red triangles).
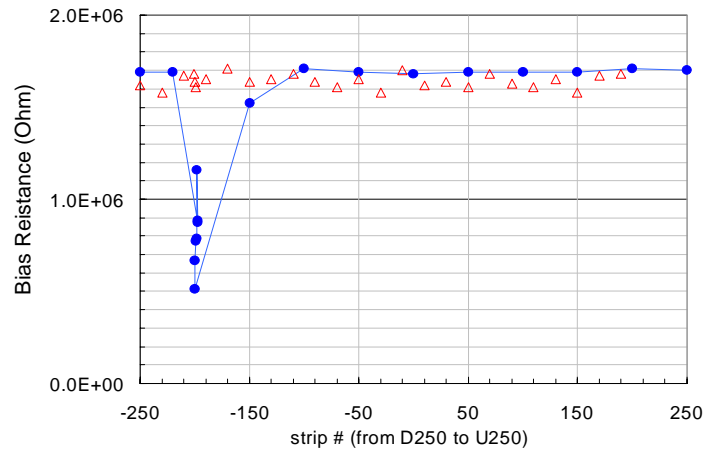
5. Conclusions

We have evaluated the electrical performance of prototype silicon sensors fabricated for the SVX2b Detector. As shown in this note and in CDF-6286, the prototypes fulfill our specifications.

Five sensors irradiated with neutrons are characterized. The performance after irradiation is consistent with characteristics previously known. Because of bulk type inversion and positive charge accumulation, we require a bias voltage of typically 200V (full depletion is about 50V) for the sensors irradiated to $0.7 \times 10^{14}/cm^2$ and 300-350V (full depletion is 130V) for those irradiated to $1.4 \times 10^{14} n/cm^2$ in order to accomplish the best electrical performance.

We have addressed susceptibility of sensors against charge-up. It seems this susceptibility is degraded with time and the effect should diminish when the sensors are wire-bonded to ASICs. We need to pay attention not to create charge-up.

Appendix. Equations used to calculate evolution of full depletion voltage

The full depletion voltage of silicon sensor with thickness of d is given by

$$V_{FD} = \frac{\left|N_{eff}\right|ed^2}{2\varepsilon}$$

under planer diode assumption. Here permittivity of silicon is $\varepsilon = 11.9 \times 8.85 \times 10^{-14}$ F/cm. The same equation is used to calculate the initial impurity density $N_{eff\,0}$ using the initial full depletion voltage (150 V).

The initial n type impurity density decreases with radiation (and time) since new levels of displacement damages induced by radiation act as effectively p type:

$$N_{eff} = N_{eff\,0} - N_{damage}(\phi, t, T)$$

The radiation effects can be classified into three types.

$$N_{damage}(\phi, t, T) = N_c(\phi) + N_a(\phi, t, T) + N_Y(\phi, t, T)$$

The first effect is stable damage, representing increase of donor type impurities and creation of acceptor type impurities, which is expressed by the following equation:

$$N_c(\phi) = N_{c0}\left(1 - \exp(-c\phi)\right) + g_c\phi$$

The fraction N_{c0}/N_c refers to "incompleteness" in donor removal.

The second effect is short-term annealing after irradiation.

$$N_a(\phi, t, T) = g_a\phi \exp\left(-k_{a0}t \exp\left(-E_{aa}/k_B T\right)\right)$$

where the model assumes activation energy E_{aa} and time constant k_{a0}.

The last effect is long-term reverse annealing:

$$N_Y(\phi, t, T) = g_Y\phi\left(1 - \frac{1}{1 + k_{Y10}t\exp(-E_{aY}/k_B T)}\right)$$

The parameters used in the calculation are listed below.

$N_{c0} = 0.65 N_{eff\,0}$

$c = 1.1 \times 10^{-13}\,\text{cm}^2$

$g_c = 1.49 \times 10^{-2}\,\text{cm}^{-1}$

$g_a = 1.81 \times 10^{-2}\,\text{cm}^{-1}$

$g_Y = 5.16 \times 10^{-2}\,\text{cm}^{-1}$

$k_{a0} = 2.4 \times 10^{13}\,\text{s}^{-1}$

$k_{Y10} = 1.5 \times 10^{15}\,\text{s}^{-1}$

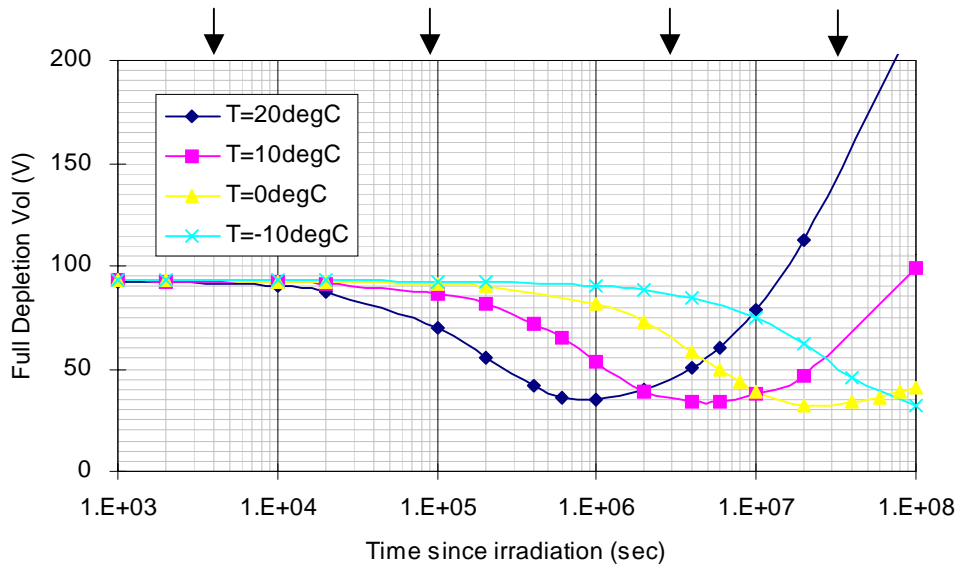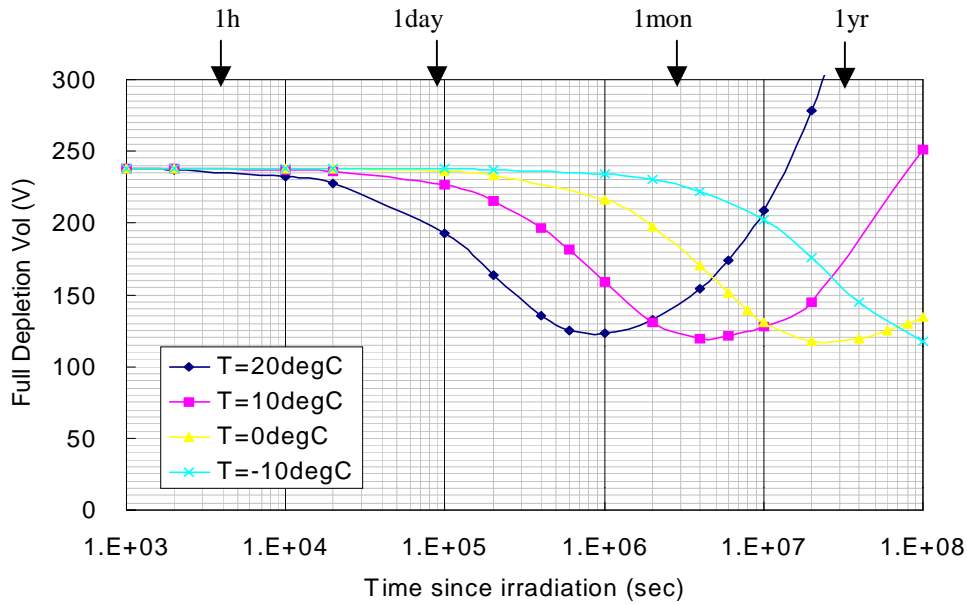$E_{aa} = 1.09\,\text{eV}$

$E_{aY} = 1.33\,\text{eV}$

Fig. 12c Evolution of full depletion voltage since completion of irradiation. Parameters are taken from ROSE Collaboration. Initial full depletion voltage 150V, and neutron fluence 0.7×10^{14} /cm^2.

Similar to Fig. 11e, but for neutron fluence 1.4×10^{14} /cm^2